JOC Article

A Computational Study of Lithium Ketone Enolate Aggregation in the Gas Phase and in THF Solution

Lawrence M. Pratt*

Department of Chemistry, Fisk University, 1000 17th Avenue North, Nashville, Tennessee 37208

Son C. Nguyen and Bui T. Thanh

Department of Chemistry, University of Science, Vietnam National University, 227 Nguyen Van Cu, District 5, Ho Chi Minh City, Vietnam

lpratt@fisk.edu

Received March 7, 2008

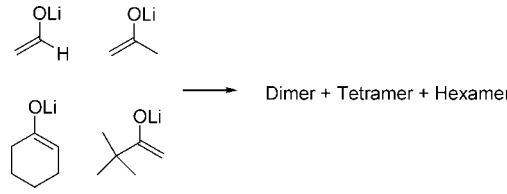

The aggregation state of several lithium enolates were calculated in the gas phase and in THF solution by the B3LYP DFT and MP2 methods. The gas phase free energies of aggregate formation were underestimated by the DFT calculations, compared to those obtained by the G3MP2 method, although DFT did correctly predict the hexamer to be the major gas phase species. The DFT calculations correctly predicted the tetramer to be the major species in THF, while MP2 underestimated the stability of the tetramer relative to the dimer.

Introduction

Lithium enolates are among the most important reagents for carbon−carbon bond formation in organic synthesis.[1,2] Like most other organolithium compounds they exist as aggregates in solution and the solid state. Several methods have been used to determine the aggregation state of organolithium compounds, including colligative property measurements, ultraviolet spectroscopy, NMR spectroscopy, and computational methods.[3,4] The latter have evolved from the use of semiempirical calculations common during the 1980s and 1990s to more accurate density functional theory (DFT) methods and ab initio calculations that are in common use today. With significant advances in computer hardware and software, it is often possible to approach chemical accuracy with molecular modeling studies.

A great deal is now known about the solution structure of lithium dialkylamides thanks to $^{6}Li-^{15}N$ double labeling NMR studies. Major advances in this area were the subject of a review.[5] Determination of the aggregation state of lithium enolates has been more challenging because a nonquadrupolar, NMR active isotope of oxygen is not available, and indirect methods for structure determination are often used. An unsolvated hexameric lithium enolate of lithioisobutyrophenone has been observed by X-ray crystallography.[6] A similar hexameric solid state structure has been reported for the lithium enolate of *tert*-butyl methyl ketone (pinacolone).[7,8] Although the solution structures of lithium compounds are not necessarily the same as those of the solid state structures, X-ray structures do give a good picture of trends. Discrepancies between the solution and solid state structures are expected when the energy differences between different aggregates are small. Analogous hexameric ester enolates have been observed by X-ray crystallography in the solid state, and deduced from ^{6}Li NMR by observing the resonances in an ensemble of diastereomeric aggregates in a solution of the racemic enolate.[9] THF solvated lithium enolates generally form tetrameric structures. A crystal structure of the lithium enolate of pinacolone (MTBK) was found to consist of a tetramer with one THF ligand on each

(1) Woltermann, C. J.; Hall, R. W.; Rathman, T. *PharmaChem* **2003**, *2*, 4.
(2) Berrisford, D. J. *Angew. Chem., Int. Ed. Engl.* **1995**, *34*, 178.
(3) Pratt, L. M. *Res. Adv. Org. Chem.* **2003**, *3*, 13.
(4) Pratt, L. M. *Mini Rev. Org. Chem.* **2004**, *1*, 209.
(5) Collum, D. B. *Acc. Chem. Res.* **1993**, *26*, 227.
(6) Nichols, M. A.; Leposa, C. M.; Hunter, A. D.; Zeller, M. *J. Chem. Crystalogr.* **2007**, *37*, 825.
(7) Williard, P. G.; Carpenter, G. B. *J. Am. Chem. Soc.* **1985**, *107*, 3345.
(8) Williard, P. G.; Carpenter, G. B. *J. Am. Chem. Soc.* **1986**, *108*, 462.
(9) McNeil, A. J.; Toombes, G. E. S.; Gruner, S. M.; Lobkovsky, E.; Collum, D. B.; Chandramouli, S. V.; Vanasse, B. J.; Ayers, T. A. *J. Am. Chem. Soc.* **2004**, *126*, 16559.

10.1021/jo800528y CCC: $40.75
Published on Web 07/23/2008

lithium atom.[10] Lithium enolates of acetaldehyde, isobutyrophenone, and α-tetralone were reported as tetramers in THF solution based on NMR spin lattice relaxation times.[11–13] Lithium enolate tetramers were also observed in THF by Collum and co-workers using the method of continuous variation with an ensemble of heteroaggregates.[14] In very dilute THF solutions, monomers, dimers, and tetramers of ketone enolates have been reported.[15–17]

Early computational studies of organolithium compounds frequently used the MNDO or PM3 semiempirical methods, which are now largely obsolete for all but the largest systems. Early studies on lithium enolates and their mixed aggregates used small model systems and extrapolated the findings to larger systems,[18,19] which was common practice due to the hardware and software limitations of that time. Other work focused on the full system of interest, but at low levels of theory.[20] The development of DFT methods has allowed reliable computational studies to be performed on the full systems of interest, including solvating ligands. Solvent effects can be modeled either by using a continuum model or by explicitly incorporating solvent ligands into the molecule, which we refer to as microsolvation. The resulting supermolecule is used to represent the organolithium monomer or aggregate with its inner solvation sphere. This method has proven superior to continuum solvent models for organolithium compounds, which cannot account for the steric effects of coordinated solvent ligands.[21,22] Our calculations over the past several years showed that in spite of similar steric effects, dimethyl ether is a poor substitute for THF, resulting in errors in aggregation energies of several kilocalories per mole.[23,24] With use of THF ligands in the models, DFT calculations have provided at least qualitatively correct aggregation states for alkyllithiums,[25] lithium dialkylamides,[26] and lithium dialkylamide−lithium chloride mixed aggregates[27] in THF solution.

DFT methods are imperfect, however. They often underestimate reaction barrier heights in an unpredictable manner.[28] They sometimes fail to correctly predict the energy and geometry for systems with a flat potential energy surface.[29] We recently found that the popular B3LYP functional predicts the free energies of successive THF solvation of organolithium compounds to be too endergonic when compared to higher level computational methods.[30] This appears to be a systematic error, however, and with an appropriate correction factor, reliable estimates of the solvation state can be obtained.

To our knowledge a systematic computational investigation of the solvation and aggregation states of lithium ketone enolates has not yet been performed. The purpose of this paper is to determine the effects of increasing steric bulk on the aggregation of these species and to evaluate the performance of the B3LYP functional by comparison to more accurate ab initio methods for sufficiently small molecules. Beginning with the lithium enolate of acetaldehyde (**1**), the enolate size was increased as the enolates of acetone (**2**), cyclohexanone (**3**), and *tert*-butyl methyl ketone (MTBK, **4**) were modeled.

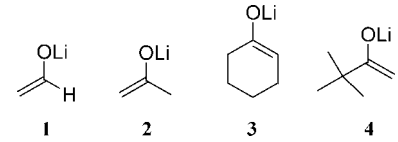

1 **2** **3** **4**

Computational Methods

All calculations were performed with Gaussian 03.[31] All geometries were optimized at the B3LYP/6-31+G(d) level, followed by frequency calculations at the same level of theory. Selected molecules were reoptimized at the MP2/6-31+G(d) level, and the B3LYP thermal corrections were added to the MP2 electronic energies to obtain approximate free energies. In addition, free energies for selected molecules were also calculated with the highly accurate G3MP2 method,[32] which includes Hartree−Fock thermal corrections. This method uses a series of calculations to approximate the results of high-level calculations. Several studies have shown that the G3MP2 method generates accurate enthalpies and free energies of formation for a diverse set of organic molecules.[33–35] The gas phase and solution energies reported include gas phase internal energy and thermal corrections to the free energy at 200 and 298.15 K. The lithium enolates and their inner solvation sphere of coordinated THF ligands were taken as a "supermolecule" and used to represent the enolates in THF solution. Strictly speaking, these are still gas phase species, and correction terms are normally needed to convert the gas phase free energies to standard state of a solution, which is taken as 1 mol L^{-1}. The details of these corrections have been previously published.[36] Yet another correction is required for proper treatment of the explicit solvent molecules used in microsolvation. The traditional approach is to set the

(10) Amstutz, R.; Schweizer, W. B.; Seebach, D.; Dunitz, J. D. *Helv. Chim. Acta* **1981**, *64*, 2617.
(11) Wen, J. Q.; Grutzner, J. B. *J. Org. Chem.* **1986**, *51*, 4220.
(12) Jackman, L. M.; Szeverenyl, N, M. *J. Am. Chem. Soc.* **1977**, *99*, 4954.
(13) Jackman, L. M.; Scarmoutzos, L. M.; DeBrosse, C. W. *J. Am. Chem. Soc.* **1987**, *109*, 5355.
(14) Liou, L. R.; McNeil, A. J.; Ramirez, A.; Toombes, G. E. S.; Gruver, J. M.; Collum, D. B. *J. Am. Chem. Soc.* **2008**, *130*, 4859.
(15) Streitwieser, A.; Wang, D. Z.-R. *J. Am. Chem. Soc.* **1999**, *121*, 6213.
(16) Wang, D. Z.-R.; Kim, Y.-J.; Streitwieser, A. *J. Am. Chem. Soc.* **2000**, *122*, 10754.
(17) Streitwieser, A.; Juaristi, E.; Kim, Y.-J.; Pugh, J. K. *Org. Lett.* **2000**, *2*, 3739.
(18) Pratt, L. M.; Streitwieser, A. *J. Org. Chem.* **2003**, *68*, 2830.
(19) Abbotto, A.; Streitwieser, A.; Schleyer, P. v. R. *J. Am. Chem. Soc.* **1997**, *119*, 11255.
(20) Weiss, H.; Yakimansky, A. V.; Muller, A. H. *J. Am. Chem. Soc.* **1996**, *118*, 8897.
(21) Pratt, L. M.; Mogali, S.; Glinton, K. *J. Org. Chem.* **2003**, *68*, 6484.
(22) Pratt, L. M.; Ramachandran, B.; Xidos, J. D.; Cramer, C. J.; Truhlar, D. G. *J. Org. Chem.* **2002**, *67*, 7607.
(23) Pratt, L. M.; Mu, R.; Jones, D. R. *J. Org. Chem.* **2005**, *70*, 101.
(24) Pratt, L. M.; Mu, R. *J. Org. Chem.* **2004**, *69*, 7519.
(25) Pratt, L. M.; Truhlar, D. G.; Cramer, C. J.; Kass, S. R.; Thompson, J. D.; Xidos, J. D. *J. Org. Chem.* **2007**, *72*, 2962.
(26) Pratt, L. M. *THEOCHEM* **2007**, *811*, 191.
(27) Pratt, L. M. *Bull. Chem. Soc. Jpn.* **2005**, *78*, 890.
(28) Pratt, L. M.; Nguyen, N. V.; Ramachandran, B. *J. Org. Chem.* **2005**, *70*, 4279.
(29) Pratt, L. M.; Phan Tran, D. H.; Tran, P. T. T.; Nguyen, N. V. *Bull. Chem. Soc. Jpn.* **2007**, *80*, 1587.
(30) Pratt, L. M.; Jones, D.; Sease, A.; Busch, D.; Faluade, E.; Nguyen, S. C.; Thanh, B. T. *Int. J. Quantum Chem.* **2008**, in press.
(31) Frisch, M. J.; Trucks, G. W.; Schlegel, H. B.; Scuseria, G. E.; Robb, M. A.; Cheeseman, J. R.; Montgomery, J. A., Jr.; Vreven, T.; Kudin, K. N.; Burant, J. C.; Millam, J. M.; Iyengar, S. S.; Tomasi, J.; Barone. V.; Mennucci, B.; Cossi, M.; Scalmani, G.; Rega, N.; Petersson, G. A.; Nakatsuji, H.; Hada, M.; Ehara, M.; Toyota, K.; Fukuda, R.; Hasegawa, J.; Ishida, M.; Nakajima, T.; Honda, Y.; Kitao, O.; Nakai, H.; Klene, M.; Li, X.; Knox, J. E.; Hratchian, H. P.; Cross, J. B.; Adamo, C.; Jaramillo, J.; Gomperts, R.; Stratmann, R. E.; Yazyev, O.; Austin, A. J.; Cammi, R.; Pomelli, C.; Ochterski, J. W.; Ayala, P. Y.; Morokuma, K.; Voth, G. A.; Salvador, P.; Dannenberg, J. J.; Zakrzewski, V. G.; Dapprich, S.; Daniels, A. D.; Strain, M. C.; Farkas, O.; Malick, D. K.; Rabuck, A. D.; Raghavachari, K.; Foresman, J. B.; Ortiz, J. V.; Cui, Q.; Baboul, A. G.; Clifford, S.; Cioslowski, J.; Stefanov, B. B.; Liu, G.; Liashenko, A.; Piskortz, P.; Komaromi, I.; Martin, R. L.; Fox, D. J.; Keith, T.; Al-Laham, M. A.; Peng, C. Y.; Nanayakkara, A.; Challacombe, M.; Gill, P. M. W.; Johnson, B.; Chem, W.; Wong, M. W.; Gonzalez, C.; Pople, J. A. *Gaussian 03*, Revision A.1; Gaussian, Inc.: Pittsburgh, PA, 2003.
(32) Curtiss, L. A.; Redfern, P. C.; Raghavachari, K.; Rassolov, V.; Pople, J. A. *J. Chem. Phys.* **1999**, *110*, 4703.
(33) Emel'yanenko, V. N.; Toktonov, A. V.; Kozlova, S. A.; Verevkin, S. P. *J. Phys. Chem. A* **2008**, *112*, 4036.
(34) Islam, S. M.; Poirier, R. A. *J. Phys. Chem. A* **2007**, *111*, 13218.
(35) Bond, D. *J. Org. Chem.* **2007**, *72*, 7313.
(36) Pratt, L. M.; Merry, S.; Nguyen, S. C.; Quan, P.; Thanh, B. T. *Tetrahedron* **2006**, *62*, 10821.

standard state of a pure liquid to be the concentration of the pure liquid itself, which then allows one to drop the concentration of the pure liquid from equilibrium expressions (consider the ionic product of water, for example). However, since we have decided to adopt the standard state of 1 mol L^{-1} for all species, the free energy change for the process

$$2\,\mathrm{RLi}\bullet 2\,\mathrm{THF} \rightarrow (\mathrm{RLi}\bullet \mathrm{THF})_2 + 2\,\mathrm{THF} \qquad (1)$$

is given by[37]

$$\Delta G^\circ = -RT\ln\frac{[(\mathrm{RLi}\bullet \mathrm{THF})_2]}{[\mathrm{RLi}\bullet 2\,\mathrm{THF}]^2} - 2RT\ln[\mathrm{THF}] \qquad (2)$$

The molarity of the THF solvent was calculated to be 13.26 at 200 K, and 12.33 at 298.15 K, from its tabulated density.[38] The corrections due to the second term in the equation above amount to −1.0273 and −1.4883 kcal/mol per THF at 200 and 298.15 K, respectively. These corrections were included whenever free THF appeared on one side of the equation. Thus, when a mole of free THF appears on the right side of the equation, the equilibrium is shifted to the side of the reactants, and vice versa.

Results and Discussion

The free energies of aggregate formation in the gas phase were calculated according to eqs 3–5. The data in Table 1 compare the free energy of lithium acetaldehyde enolate aggregate formation at the B3LYP/6-31+G(d), MP2/6-31+G(d), and G3MP2 levels. The dimerization energy was calculated for the syn-dimer, which was the most stable form of the acetaldehyde enolate. The other enolates, described below, favored the anti conformation in the gas phase. The free energies of dimer formation were within 4 kcal/mol of each other using the three computational methods. For tetramer formation, the MP2 and G3MP2 results were similar, but the B3LYP free energy was less exergonic than the G3MP2 by nearly 8 kcal/mol. A recent study of lithium carbenoid dimerization energies found the G3MP2 energies to be in good agreement with those obtained at the CCSD(T)/aug-cc-pvdz//MP2/aug-cc-pvdz level.[29] Taking the G3MP2 energies as the best available, the MP2 energies were slightly too negative but in better agreement than those calculated at the B3LYP level.

$$2\,\mathrm{Monomer} \rightarrow \mathrm{Dimer} \qquad (3)$$

$$2\,\mathrm{Dimer} \rightarrow \mathrm{Tetramer} \qquad (4)$$

$$^3/_2\,\mathrm{Tetramer} \rightarrow \mathrm{Hexamer} \qquad (5)$$

The optimized geometries of the gas phase aggregates of the acetaldehyde enolate are shown in Figure 1. The monomer optimized to a geometry in which the lithium was coordinate to the oxygen and two carbon atoms, which is consistent with the global minimum reported by Houk and co-workers.[39] The other lithium enolates optimized to similar structures, which are provided in the Supporting Information. The free energies of aggregate formation, calculated at the B3LYP/6-31+G(d) level, are shown in Table 2. Although this method predicts aggregation energies to be the least endergonic of the three methods, it still predicts the hexamer to be the predominant form in the gas phase, which will likely be similar to the situation in nonpolar solvents such as hexane. This is consistent with the limited experimental data available, which showed lithioisobutyrophenone and pinacolone to be hexameric in the solid state.[6–8]

TABLE 1. Calculated Free Energies (kcal/mol, Eqs *3–5*) of Lithium Acetaldehyde Enolate Aggregate Formation at 298.15 K

method	dimer	tetramer	hexamer
B3LYP/6-31+G(d)	−41.0	−33.2	−12.6
MP2/6-31+G(d)	−44.5	−44.3	−16.7
G3MP2	−42.5	−41.0	

TABLE 2. Gas Phase Free Energies of Aggregate Formation (kcal/mol) Calculated at the B3LYP/6-31+G(d) Level

Li enolate of	temp (K)	dimer	tetramer	hexamer
acetaldehyde	200	−44.2	−37.3	−15.6
acetaldehyde	298.15	−41.0	−33.2	−12.6
acetone	200	−44.0	−34.9	−16.4
acetone	298.15	−40.6	−30.0	−14.3
cyclohexanone	200	−45.1	−36.4	−17.7
cyclohexanone	298.15	−41.6	−31.8	−15.6
MTBK	200	−42.8	−30.4	−10.8
MTBK	298.15	−39.4	−25.3	−8.64

TABLE 3. Free Energies of Enolate Monomer Trisolvate Formation (kcal/mol, Eq *6*)

Li enolate of	method	200 K	298.15 K
acetaldehyde	B3LYP/6-31+G(d)	−2.59	−0.26
acetaldehyde	MP2/6-31+G(d)	−13.3	−10.4
acetone	B3LYP/6-31+G(d)	−4.43	−1.53
acetone	MP2/6-31+G(d)	−12.9	−10.0
cyclohexanone	B3LYP/6-31+G(d)	−4.78	−2.77
cyclohexanone	MP2/6-31+G(d)	−16.2	−14.2
MTBK	B3LYP/6-31+G(d)	−0.75	2.07
MTBK	MP2/6-31+G(d)	−15.8	−13.0

Before predicting the aggregation state of solvated lithium enolates, it is necessary to know the solvation state of the monomers and dimers. These were calculated according to eqs 6–8, taking into account the standard state corrections for free THF. The free energies of trisolvated monomer formation from the disolvate are shown in Table 3. The analogous free energies for tetrasolvated dimer formation from the disolvate are shown in Table 4. Compared to the MP2 calculations, the B3LYP method predicted less negative free energies of formation of the higher solvates. Based on our prior studies, the MP2/6-31+G(d) calculations are more reliable than DFT for successive solvation energies, although these may overestimate the exergonic solvation energies compared to higher level calculations by a couple of kilocalories per mole.[30] Allowing for this systematic error, the free energies for the third solvation of the monomer will still be exergonic by at least 10 kcal/mol at 200 K, and slightly less at 298 K. We therefore conclude that the lithium enolate monomers all exist as the THF trisolvate. The optimized geometries are shown in Figure 2. These structures show that the solvated enolates are bonded to the lithium atom solely via the oxygen atom, as opposed to $^3\eta$ coordination to the carbon and oxygen atoms in the gas phase.

$$\mathrm{Monomer}\bullet 2\,\mathrm{THF} + \mathrm{THF} \rightarrow \mathrm{Monomer}\bullet 3\,\mathrm{THF} \qquad (6)$$

$$\mathrm{Dimer}\bullet 2\,\mathrm{THF} + \mathrm{THF} \rightarrow \mathrm{Dimer}\bullet 3\,\mathrm{THF} \qquad (7)$$

$$\mathrm{Dimer}\bullet 3\,\mathrm{THF} + \mathrm{THF} \rightarrow \mathrm{Dimer}\bullet 4\,\mathrm{THF} \qquad (8)$$

The lithium enolate disolvated dimers could exist in the syn or anti conformations described for the gas phase structures. The lithium acetaldehyde enolate favored the syn conformation,

(37) Thompson, J. D.; Cramer, C. J.; Truhlar, D. G. *J. Chem. Phys.* **2003**, *119*, 1661.
(38) Govender, U. P.; Letcher, T. M.; Garg, S. K.; Ahluwalia, J. C. *J. Chem. Eng. Data* **1996**, *41*, 147.
(39) Houk, R. J.; Anslyn, E. V.; Stanton, J. F. *Org. Lett.* **2006**, *8*, 3461.

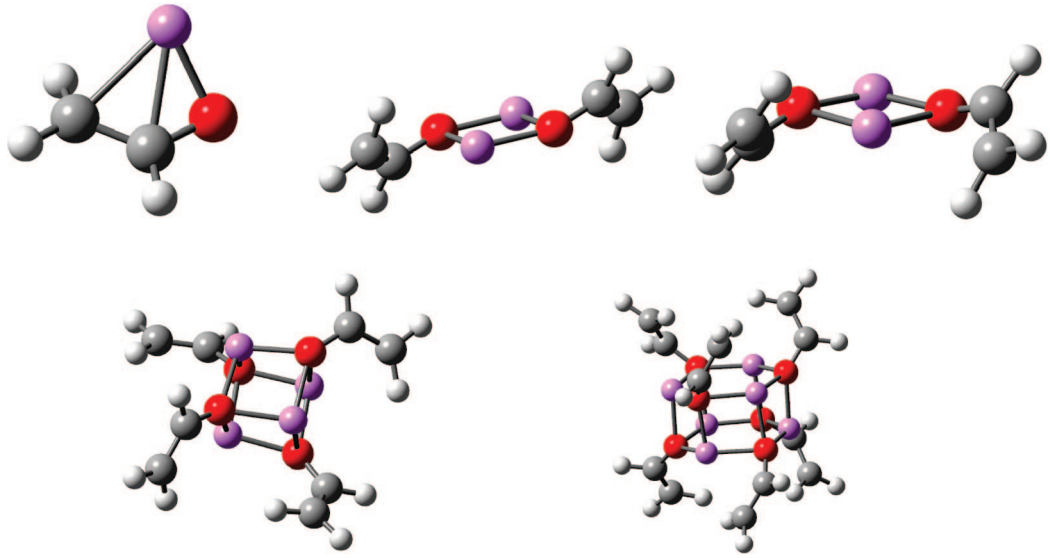

FIGURE 1. B3LYP/6-31+G(d) optimized geometries of lithium acetaldehyde enolate aggregates. Top left, monomer; top center, anti-dimer; top right, syn-dimer; bottom left, tetramer; bottom right, hexamer; gray, carbon; white, hydrogen; red, oxygen; violet, lithium.

TABLE 4. Free Energies of Enolate Dimer Tri- and Tetrasolvate Formation (kcal/mol, Eqs *7* and *8*)

		trisolvate		tetrasolvate	
Li enolate of	method	200 K	298.15	200 K	298.15
acetaldehyde syn	B3LYP/6−31+G(d)	−2.53	−0.44	−1.73	0.53
acetaldehyde syn	MP2/6-31+G(d)	−14.6	−12.6	−12.4	−10.1
acetaldehyde anti	B3LYP/6-31+G(d)	−2.51	0.074	−0.17	2.36
acetaldehyde anti	MP2/6-31+G(d)	−13.2	−10.6	−14.2	−11.7
acetone	B3LYP/6-31+G(d)	0.27	2.78	−0.12	2.75
acetone	MP2/6-31+G(d)	−12.8	−10.2	−15.1	−12.2
cyclohexanone	B3LYP/6-31+G(d)	0.081	3.39	−0.56	1.56
cyclohexanone	MP2/6-31+G(d)	−12.7	−9.44	−15.8	−13.7
MTBK	B3LYP/6-31+G(d)	1.21	3.95	4.43	7.60
MTBK	MP2/6-31+G(d)	−17.1	−14.5		

and both conformations were used in the calculations for comparison. The acetone enolate had a slight preference for the syn conformation in THF solution, and the other enolates favored the anti form.

The free energies of the tri- and tetrasolvated dimer formation were calculated at the B3LYP/6-31+G(d) and MP2/6-31+G(d) levels for the acetaldehyde and acetone enolates. The MP2 calculations predicted the addition of the third and fourth THF ligands to be more exergonic by about 12−18 kcal/mol per THF

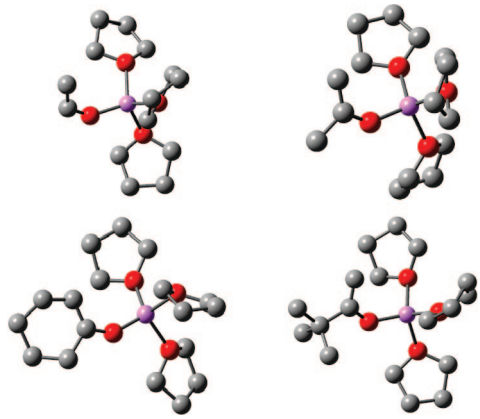

FIGURE 2. B3LYP/6-31+G(d) optimized geometries of lithium enolate trisolvated monomers. Hydrogens are omitted for clarity. Top left, acetaldehyde enolate; top right, acetone enolate; bottom left, cyclohexanone enolate; bottom right, MTBK enolate.

in comparison to the B3LYP calculations. A tetrasolvated lithium amide enolate dimer was observed in the solid state.[40] This enolate was of similar steric bulk to the ketone enolates in this study. Although the solid state structures are not necessarily the same as solution structures, they do prove that these THF tetrasolvated species can exist. We therefore conclude that the acetaldehyde, acetone, and cyclohexanone enolate dimers are tetrasolvated. Although the MTBK enolate tetrasolvated dimer is too large to optimize at the MP2 level, it will likely be tetrasolvated as well. This is the same conclusion reached by Schleyer and co-workers,[19] albeit at a lower level of theory and using dimethyl ether in their microsolvation model. The optimized geometries of the tetrasolvated enolate dimers are shown in Figure 3.

Starting with the trisolvated lithium enolate monomers and the tetrasolvated enolate dimers, the free energies of dimerization were calculated according to eq 9. The results are shown in Table 5. The results indicate that in a 1 M solution, each of the lithium enolates will exist as a dimer or a higher aggregate, with the tendency toward aggregate formation increasing with temperature. The DFT results were in qualitative agreement with the MP2 calculations. The DFT and MP2 dimerization energies were within about 3 kcal/mol of each other for each of the systems for which the MP2 energies were calculated.

$$2\,\text{Monomer}\bullet 3\,\text{THF} \rightarrow \text{Dimer}\bullet 4\,\text{THF} + 2\,\text{THF} \qquad (9)$$

The free energies of the tetrasolvated enolate tetramers were calculated from the tetrasolvated dimer (eq 10). The results are

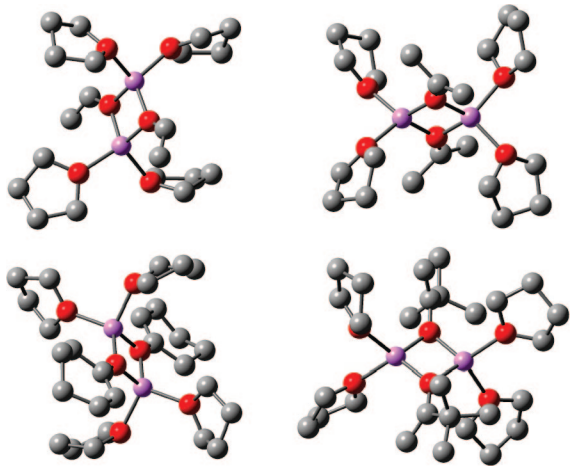

FIGURE 3. B3LYP/6-31+G(d) optimized geometries of lithium enolate tetrasolvated dimers. Hydrogens are omitted for clarity. Top left, acetaldehyde enolate; top right, acetone enolate; bottom left, cyclohexanone enolate; bottom right, MTBK enolate.

TABLE 5. Free Energies of Enolate Dimerization in THF (kcal/mol, Eq *9*)

Li enolate of	method	200 K	298.15 K
acetaldehyde syn	B3LYP/6-31+G(d)	−17.9	−20.3
acetaldehyde syn	MP2/6-31+G(d)	−14.2	−16.5
acetaldehyde anti	B3LYP/6-31+G(d)	−16.1	−17.7
acetaldehyde anti	MP2/6-31+G(d)	−13.6	−15.2
acetone	B3LYP/6-31+G(d)	−16.3	−18.2
acetone	MP2/6-31+G(d)	−15.4	−17.3
cyclohexanone	B3LYP/6-31+G(d)	−25.9	−26.8
cyclohexanone	MP2/6-31+G(d)	−24.4	−25.2
MTBK	B3LYP/6-31+G(d)	−10.5	−11.3

TABLE 6. Free Energies of Enolate Tetramer Formation from THF Tetrasolvated Dimer (kcal/mol, Eq *10*)

Li enolate of	method	200 K	298.15 K
acetaldehyde syn	B3LYP/6-31+G(d)	−14.1	−18.8
acetaldehyde syn	MP2/6-31+G(d)	8.14	3.43
acetone	B3LYP/6-31+G(d)	−14.4	−19.1
cyclohexanone	B3LYP/6-31+G(d)	−15.3	−20.2
MTBK	B3LYP/6-31+G(d)	−3.44	−7.15

shown in Table 6, and the optimized geometries of the solvated tetramers are shown in Figure 4. Starting from the tetrasolvated dimer, B3LYP predicts each of the enolates to be tetrameric in THF solution. This is consistent with the solid state structure reported by Seebach.[10] In contrast, the MP2 calculations predicted the lithium acetaldehyde enolate to be dimeric when the calculations were performed according to eq 10.

$$2\,\text{Dimer}\bullet 4\,\text{THF} \rightarrow \text{Tetramer}\bullet 4\,\text{THF} + 4\,\text{THF} \quad (10)$$

The published experimental data indicate that unsolvated lithium enolates form hexamers, and our calculations are consistent with that data at each level of theory. The B3LYP calculations underestimated the free energies of tetramer and hexamer formation relative to higher level calculations, but still predicted the hexamer to be the major unsolvated species. The situation is more complex in THF formation. Both the B3LYP and MP2 calculations predict each enolate monomer to be trisolvated by THF. The dimers are predicted to be tetrasolvated by MP2 and either di- or tetrasolvated by B3LYP. The single

(40) Bauer, W.; Laube, T.; Seebach, D. *Chem. Ber.* **1985**, *118*, 764.

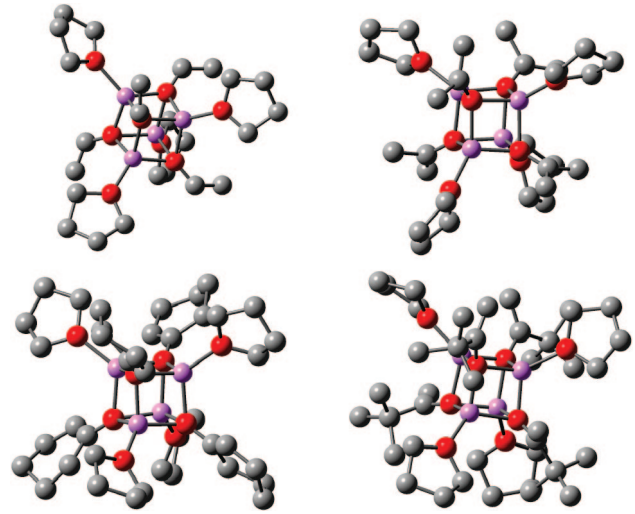

FIGURE 4. B3LYP/6-31+G(d) optimized geometries of lithium enolate tetrasolvated tetramers. Hydrogens are omitted for clarity. Top left, acetaldehyde enolate; top right, acetone enolate; bottom left, cyclohexanone enolate; bottom right, MTBK enolate.

published example of a lithium enolate dimer was tetrasolvated in the crystal structure. That fact and our prior work comparing DFT and ab initio methods[30] lead us to trust the MP2 results in this case. Thus, the prediction of the aggregation states of solvated lithium enolates is based on the trisolvated monomer, tetrasolvated dimer, and tetrasolvated tetramer.

Table 6 shows a discrepancy between the B3LYP and MP2 calculations for the aggregation state of the lithium acetaldehyde enolate. In the gas phase, the MP2 calculations predicted aggregation free energies in good agreement with the more accurate G3MP2 method, and it was superior to B3LYP for that system. On the other hand, the results in Table 6 would be expected if the MP2 method overestimated the binding energy of the THF ligands to the lithium enolate dimer, since free THF is produced during the tetramer formation. On the left side of eq 10 there are 8 Li−THF bonds, and only 4 such bonds on the right side. Our prior study[30] suggested that with a modest basis set such as 6-31+G(d), MP2 can overestimate the binding energy of THF ligands to unhindered organolithium compounds in comparison to higher levels of theory by as much as 3 kcal/mol. The size of the more sterically hindered enolates limited the level of the calculations that can be performed at this time. The published experimental work in solution and the solid state indicated that the tetramer is the primary aggregate in THF. We, therefore, concludethat the MP2 calculations underestimated the stability of the solvated tetramer relative to the tetrasolvated dimer by at least several kilocalories per mole, and that the B3LYP calculations gave results that are in qualitative agreement with experiment. The results were also in qualitative agreement with an early study that used a combination of DFT and semiempirical calculations, and also used dimethyl ether to represent THF solvation.[19]

Lower enolate aggregates have been reported in very dilute THF solutions,[15–18] and this can be qualitatively explained from eq 10. As the solution becomes more dilute, the concentration of THF increases relative to that of the enolate. This causes the equilibrium to shift to the left, toward the formation of dimer. Likewise, dilution of the dimer in eq 8 favors the formation of the monomer in dilute solution. Both of those species have been observed by ultraviolet−visible spectroscopy.[15–18]

The geometry of the lithium acetaldehyde hexamer with 6 coordinated THF ligands was optimized at the B3LYP level, and the free energy of hexamer formation was calculated according to eq 11. It was found to be endergonic by 10.7 and 14.5 kcal/mol at 200 and 298.15 K, respectively. Since formation of the hexamer is unfavorable for the acetaldehyde enolate, it would be at least as unfavorable for the more sterically hindered enolates. Thus, the B3LYP calculations were in agreement with the published experimental work, which concluded that the tetramer is the major species in THF solution.

$$^{3}/_{2}\,\text{Tetramer} \bullet 4\,\text{THF} \rightarrow \text{Hexamer} \bullet 6\,\text{THF} \qquad (11)$$

Conclusions

Both the DFT and MP2 calculations predict the lithium enolates of this study to exist as hexamers in the gas phase. The gas phase structures are expected to be similar to those in nonpolar solvents, and the gas phase calculations are in good agreement with the available experimental data for solid state and hydrocarbon solutions of lithium enolates.

The DFT calculations predict the tetrasolvated tetramer to be the major species in THF solution, which is consistent with the available experimental data. In contrast, the MP2 calculations underestimate the free energy of tetramer formation of the lithium acetaldehyde enolate relative to the tetrasolvated dimer. This may be an indication that MP2 with a modest basis set overestimates the binding energy of the THF ligands as was suggested by an earlier study.

Acknowledgment. This work was supported in part by NSF grants INT-0454045 and CHE-0643629. This research used resources of the National Energy Research Scientific Computing Center, which is supported by the Office of Science of the U.S. Department of Energy under Contract No. DE-AC03-76SF00098. The authors acknowledge the Asia Research Center and the Korea Foundation for Advanced Studies as a sponsor of the research project.

Supporting Information Available: Tables of B3LYP optimized geometries and energies of all lithium enolate structures, and an expanded version of Figure 1. This material is available free of charge via the Internet at http://pubs.acs.org.

JO800528Y